Adsorption-induced Kondo effect in metal-free phthalocyanine on Ag(111)

J. Granet,[†] M. Sicot,[*,†] I. C. Gerber,[‡] G. Kremer,[†,¶] T. Pierron,[†] B. Kierren,[†] L. Moreau,[†] Y. Fagot-Revurat,[†] S. Lamare,[§] F. Chérioux,[§] and D. Malterre[†]

†*Université de Lorraine, CNRS, IJL, F-54000 Nancy, France*

‡*Université de Toulouse, INSA-CNRS-UPS, LPCNO, 135 Avenue de Rangueil, 31077 Toulouse, France*

¶*Département de Physique and Fribourg Center for Nanomaterials, Université de Fribourg, CH-1700 Fribourg, Switzerland*

§*Univ. Bourgogne Franche-Comté, FEMTO-ST, CNRS, UFC, 15B avenue des Montboucons, F-25030 Besançon cedex, France*

November 19, 2019

Abstract

We report on the formation of a two-dimensional supramolecular Kondo lattice made of organic molecules comprising only C, N and H atoms namely metal-free phthalocyanines 2HPc ($C_{32}H_{18}N_8$) adsorbed on a Ag(111) surface. Low-temperature scanning tunneling microscopy/spectroscopy (LT-STM/STS), ultra-violet photoemission spectroscopy (UPS) and density functional theory (DFT) are used to investigate the electronic structure of the system for low molecular density and commensurate self-assemblies. Abrikosov-Suhl resonances that are characteristic of the arising of a Kondo effect are observed using both STS and UPS at low temperatures. Whereas freestanding 2HPc is a no-spin bearing molecule, it acquires an unpaired electron in

its π-conjugated lowest unoccupied molecular orbital (LUMO) upon adsorption on Ag. As a result, Kondo effect can be interpreted as arising from the interaction between this unpaired π-spin and the Ag Fermi sea. Extra side resonances are observed in STS spectra that are a manifestation of the coupling between the π electron and molecular vibrational excitations, qualifying the effect as molecular vibrational Kondo effect. The Kondo temperature T_K was shown to vary with molecular density being reduced upon self-assembly. The variation of T_K is discussed in the light of the observation of quantum confinement of Ag surface electrons. This study brings new insights in the Kondo-related physics in correlation with molecular spins and low-dimensionality. Moreover, it may open new routes to the synthesis of organic molecular spintronic devices.

I-INTRODUCTION

Molecular magnetism have attracted rising attention since molecular based magnetic materials can have many technological applications in areas such as quantum computation,[1,2] high-density data storage and spintronics.[3–7] Very early in the development of the field, metallophthalocyanines (MPc) have proven to be a priviledged class of molecules to study magnetism at the nanometer scale.[8–11] Indeed, many MPc possess unpaired electrons in the gas phase and thus have non-zero magnetic moments. Besides, bis-phthalocyanines sandwiching rare-earth ions have been shown to behave as single-molecular magnets.[12,13] Their applicative potential has already been demonstrated, for example by fabricating functional supramolecular spin valves.[14]

The attractiveness of these molecules also lies in their easy synthesis, low cost and industrial avaibility. Particularly, they can be evaporated under ultra-high vacuum (UHV) allowing the synthesis of thin films.[15] In addition, the planar geometry of their π-conjugated ligand that can lie parallel to the surface on which they are adsorbed is an asset: the flatness of MPcs allows direct hybridization with the orbitals of the underlying substrate leading to

the modification of surface properties and new exotic phenomena when in contact with various substrates such as ferromagnetic (FM) materials,[4] topological insulators, supraconductors or 2D materials.[16–18] For instance, in the case of the MPc/FM molecular spinterfaces, it has been shown that the addition of MPc increases or invert the FM spin-polarization which is a key property regarding performance of spin devices.[19–22] In the case of CoPc/Bi_2Se_3, Caputo *et al.* have evidenced by angular-resolved photoelectron spectroscopy (ARPES), the modification of the topological surface states and the energy shift of the Dirac cone due to charge transfer from the molecule to the surface[23]. When in contact with superconductors, magnetic nano-objects can be envisaged as qubits for quantum computing devices. In such cases, the governing factor is the strength of spin-superconductor interactions. MPc/Pb(111) interfaces have been shown to be ideal platforms to tune locally this magnetic interaction strength by adsorbing the molecules on different sites or by continuously varying it using the interaction with an STM tip.[24,25] Finally, optical measurements of MPc/MoS_2 heterojunctions evidenced charge transfer that is sensitive to the transition metal core. This property allows for tuneable optical absorption making those systems interesting for optoelectronic applications.[16]

Moreover, this flat-lying molecular adsorption configuration offers an open area to the vacuum side. This gives the opportunity to manipulate the spin-state using on-top adsorption of alkali atoms or molecules to induce electron doping. Such studies have led to the emerging research field of on surface-magnetochemistry.[26,27]

In many cases, interfacial properties result from the hybridization of the highly directional d_{z^2}-orbital of the core metal atom with those of the substrate. Yet, for other MPc/inorganic interfaces, coupling can arise from hybridization with the π (p_z) orbital of the Pc ligand, as well. The filling of the π-orbital by charge transfer modifies the spin state of the molecule in comparison with the free one. As an example, it was shown that the no-spin bearing NiPc molecule acquires a $1/2$-spin of π-origin due to charge transfer upon adsorption on a Ag(100) single-crystalline surface.[28,29] This has been demonstrated by revealing the spectral

signature which is typical of a 1/2-spin object in interaction with an electron bath namely an Abrikosov-Suhl resonance of the differential conductance in the vicinity of the Fermi level E_F using LT-STM/STS resulting from Kondo effect.[30–35] On the same Ag(100) surface, CuPc which possesses a 1/2-spin state in its ground state, acquires an extra π-electron. In this last case, the molecule behaves as a two-spin system in contact with conduction electrons leading to an interesting many-body phenomenon: a triplet-singlet Kondo effect.[28] Alternatively, STM and UPS measurements recorded on the CoPc/Ag(111) interface have unravelled another more complex donation/backdonation scenario: electron injection occurs from the Ag substrate to the Co-3d orbitals that is accompagnied with a back donation of electrons from the π-orbitals to the substrate.[36]

Recently, it was shown by UPS that the metal-free phthalocyanine 2HPc which is a no-spin bearing molecule in the gas phase can also become charged upon adsorption on Ag(111).[37–39] We can therefore wonder if this system could also exhibit a Kondo effect as in the case of NiPc or CuPc on Ag(100). The implication of such a result would be that a purely organic phthalocyanine adsorbed on a silver surface could give rise to interesting magnetic properties without the involvement of 3d transition metal nor 4f rare-earth central ions as in previous studies. Indeed, only very few examples of pure organic systems presenting Kondo effect have been reported so far.[40–45]

Despite the increasing attention devoted to the abovementioned hybrid MPc/inorganic interfaces, however the spin-polarized electronic properties of the 2HPc/Ag(111) interface had been underlooked.[37–39,46] Yet, this particular system could provide a means of investigating many-body phenomena such as Kondo effect in many aspects, *e.g.* its intensity, spatial extension,[47] quantum criticality[44] when a 1/2 spin in π orbital is involved rather than a 3d or 4f-orbital. It would therefore broaden our knowledge on magnetism as well as on many-body physics at the nanometer scale and at low dimensionality.[40–43,47–62] Moreover, as illustrated above, a full description of the hybrid interfaces must necessarily consider both interfacial sides. On the metal side, sizeable modifications can also be expected as already observed

with other π-conjugated molecules at the interface with copper or silver surfaces.[39,63–67] In the case of Ag(111), it has been shown that upon molecular adsorption, an interfacial state forms originating from the hybridization of molecular orbitals with the well-known metal Shockley state.[39,68,69] Those hybrid interfacial states (HIS) are of particular importance for the understanding of contact in organic semiconductor devices and their origin are not yet fully understood[63,67]. Therefore, such a study might also unravel insights on the Ag hybrid interface state.

In this framework, we have investigated by LT-STM/STS, UPS and DFT, the electronic structure of adsorbed 2HPc on Ag(111) for single molecules as well as for two-dimensional self-assembled molecular networks. We demonstrate the emergence of a Kondo effect regardless of the coverage in the submonolayer regime which its origin lies in the π-*sp* hybridization in agreement with the charge transfer observed in previous works and also revealed by our UPS and DFT calculations. We think that this kind of hybrid interface with molecules comprising only C, H and N-atoms may thus be envisaged to design metamaterials composed of abundant and environmental-friendly compounds.

II-METHODS

The experiments were carried out in two ultra-high vacuum systems with a base pressure of 1×10^{-10} mbar. One was equipped with a low-temperature Omicron STM operating at 5 K. The other one was equipped with a ScientaOmicron DA30-L hemispherical analyzer and a monochromatized He_I ($h\nu = 21.2$ eV) UV source for ARPES. As beam damage of the molecular layers was observed on a timescale of about 20 min, duration of the measurements and sample position were adjusted accordingly. Due to angular distribution of the photoemission intensity, ultra-violet photoemission spectra were recorded at an emission angle of 45°.[54,70,71] Note that, in this geometry, the Shockley surface state of Ag(111) lying in the L-gap around the Γ point of the surface Brillouin zone is not detected[69]. All spectra were normalized to

the count rate at the binding energy of 0.4 eV. LEED was available on both UHV set-ups to characterize structural properties at a sample temperature of 80 K. The Ag(111) single crystal was cleaned by repeated cycles of Ar^+ sputtering at an energy of 1 keV followed by an annealing to 800 K. 2HPc molecules were purchased from Aldrich and purified by column chromatography (silica gel, dichloromethane) prior to use. They were evaporated from a Knudsen cell at 565 K onto the sample held at room temperature. The STM images were recorded at a tunneling current I_t and a bias voltage V_b where the sign corresponds to the voltage applied to the sample. STS was acquired with a PtIr scissors-cut tip and a lock-in detection in open feedback loop conditions at a frequency of 1100 Hz and a peak-to-peak bias voltage modulation for high-resolution STS of 5 mV.

The electronic structures were obtained from DFT calculations with the VASP package[72–75] which uses the plane-augmented wave scheme[76,77] to treat core electrons. Perdew-Burke-Ernzerhof (PBE) functional[78] was used as an approximation of the exchange-correlation electronic term, but PBE-D3 scheme[79,80] was used firstly to optimize the geometry since Huang *et al.* have addressed the importance of van der Waals corrections when dealing with Pc-metallic surfaces interactions.[81] The kinetic energy cutoff was set to 400 eV, with a gaussian smearing of 0.05 eV and using a 2×2×1 k-points grid to optimize the structures with a convergence force criterium of 0.01 eV/Å for all allowed atoms to relax. For density of states (DOS) determinations, a 3×3×1 k-points grid was used in conjunction with the tetrahedron method with Blöchl corrections scheme.[82] We have confirmed that a 12 layers-slab with a vacuum height of more than 20 Å was necessary to describe accurately the intrinsic Shockley surface state of the Ag (111) surface,[83] see Fig.6 for a band structure representation in the Supporting Information. As expected, two surface states are provided by the slab approach and the average energy of the two surface states (−86 meV) is relatively close to the experimental energy value (−63 meV).[69] To mimic the individual molecule case, as well as to describe the C-phase, see definition below, a (7×7) and commensurate ([5 0; 3 6]) cell was

used respectively.

III-STRUCTURAL PROPERTIES

The growth of 2HPc on Ag(111) in the submonolayer regime has been studied in previous works. Three distinct phases form as a function of the coverage.[38] For self-assemblies, the unit cells have been determined.[38] Yet, the adsorption geometry and especially the azimuthal orientation of the molecules has only succinctly been addressed and remains elusive, particularly in self-assemblies. Nevertheless, this information is of paramount importance to elucidate the electronic properties of the metal-organic interface. Thanks to STM images with intramolecular resolution, we were able to tackle this key point as will be explained below.

According to Kröger *et al.*, at low molecular densities, 2HPc form disordered gas-like phases, referred as G-phases where the intermolecular distance changes with coverage due to substrate-mediated intermolecular repulsive interaction.[38] Upon increasing coverages to 0.5-0.89 monolayers at low temperature, they form a commensurate phase with the substrate referred as C-phase, characterized by a nearly-square unit cell which epitaxy matrix is $[5\,0;3\,6]$.[38] Our LEED patterns displayed in Fig.1(a) and Fig.2(a) are in line with those previous results. Sperl *et al.* showed that 2HPc adsorb flat onto the Ag(111) substrate *i.e.* the Pc ligand plane adsorbs parallell to the surface plane.[46] The line formed by the two pyrrolic hydrogen atoms inside the porphyrazine core which will be referred to "the 2H-axis" hereafter, was shown to be azimuthally oriented perpendicular to $\langle 01\bar{1}\rangle$ cristallographic directions of the substrate. This was later confirmed by Kügel *et al.*[84] In C-phase, Bai *et al.* measured by STM an azimuthal angle between one vector of the unit cell and the molecular axis of about $60^\circ \pm 3^\circ$ without specifying the orientation of the 2H-axis.[85] In the present work, we determine the orientation of single molecules by comparing their STM appearance

in Fig.1(b) with the HOMO of the singly charged 2HPc anion calculated in ref.[86] for which the splitted lobes are perpendicular to the 2H-axis. The specific choice of comparison with the anion is justified by the fact that the molecule gets negatively charged when adsorbed as we will discuss below. The direction of the 2H-axis of the molecules is highlighted by blue lines in Fig.1(b). Our STM images reveal that 2HPc not only adsorb with 2H-axis perpendicular to $\langle 01\bar{1}\rangle$ directions (i.e. along $\langle 2\bar{1}\bar{1}\rangle$ directions) as observed in litterature[46,84] but also parallell (within an angle error of $\pm 2°$). See for example, the two molecules marked as C' and C, respectively in Fig. 1(b). In their recent work, Kügel and coworkers demonstrate that the only way to obtain a 2H-axis along one of the $\langle 01\bar{1}\rangle$ direction is to start with a molecule which 2H-axis is perpendicular to one $\langle 01\bar{1}\rangle$ direction and induce tautomerization by applying a bias voltage pulse U such that $|U| > 0.45\,\mathrm{V}$ when the tip is located above the molecule. It is claimed that the absence of 2H-axis along $\langle 01\bar{1}\rangle$ directions can be explained by a high difference in energy with the configuration where the 2H-axis lies perpendicular to $\langle 01\bar{1}\rangle$.

On the contrary, in our work, we find two adsorption orientations that can simply be explained by molecules that could rotate in the ligand plane. Fig.1(d,e) displays the two simulated most stable adsorption configurations α and β corresponding to 2H perpendicular and parallell to $\langle 01\bar{1}\rangle$ directions, respectively in good agreement with our observations. The difference of adsorption energy between these two geometries of minimum energy is only of about 0.2 eV. From these models, one can see that the transition from one geometry to the other can occur simply via a rotation of the molecule by 30°. In our work, we found compelling evidences that such rotation can happen. In Fig.7 in the Supporting Information, two time sequences issued from pairs of STM images recorded successively show molecules that rotate without external stimuli other than the scanning tip governed by the tunneling parameters V_b, I_t with V_b much smaller than the bias voltage threshold necessary to induce tautomerization. For the particular coverage shown in Fig.1(b), the ratio of parallell to per-

pendicular configurations is 1/3 leading to the conclusion that the perpendicular geometry is the most stable one.

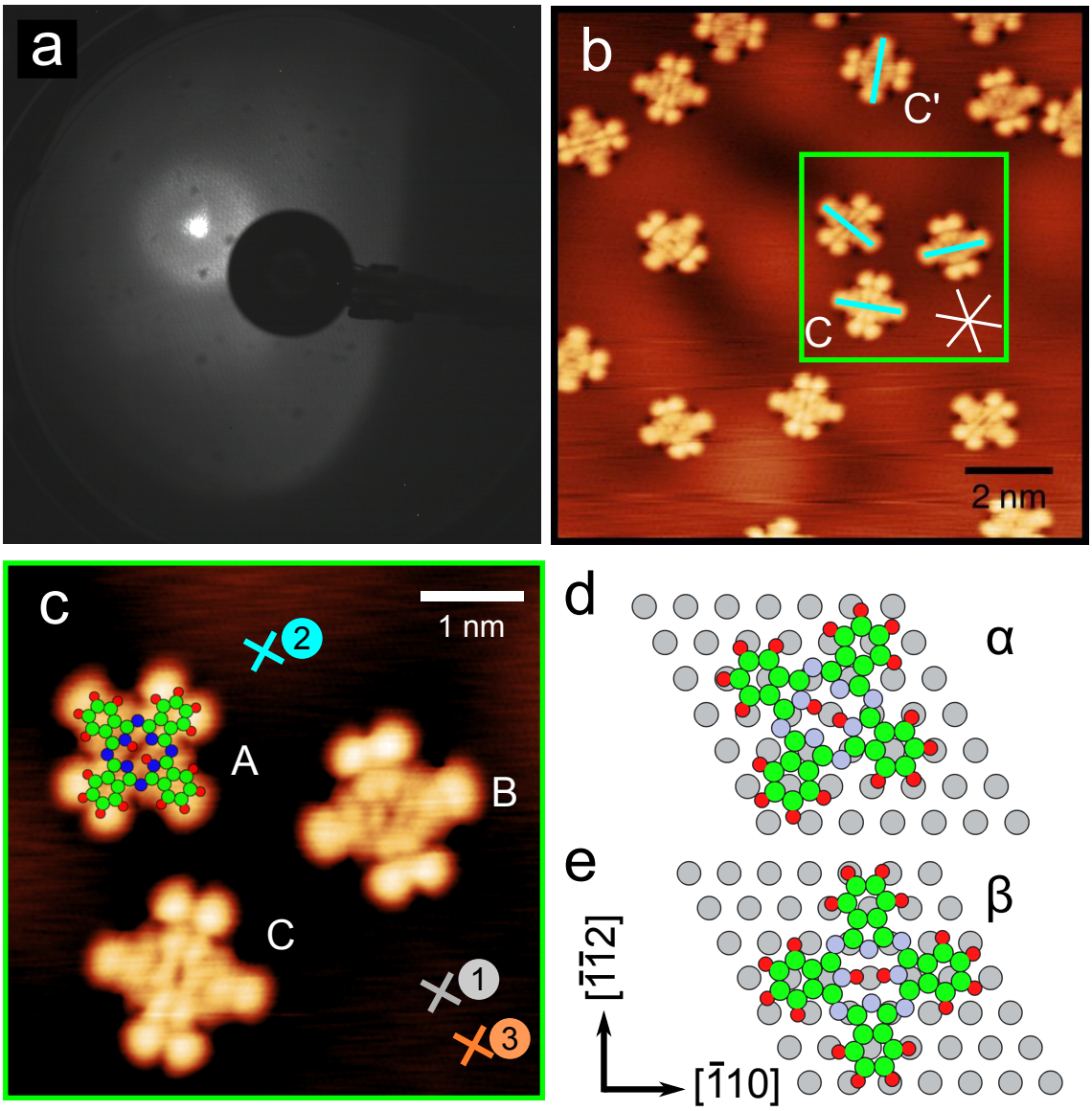

Figure 1: **The Structure of 2HPc/Ag(111) in G-phase**. (a) LEED pattern recorded at an electron energy of 15 eV. (b,c) High-resolution STM topographic images of 2HPc molecules on Ag(111). Tunneling bias conditions: $V_b = 1\,mV$, $I_t = 200\,pA$. The close-packed $\langle 01\bar{1} \rangle$ directions of the Ag(111) are indicated by white lines in (b). The numbered crosses in (c) indicates the location where the STS spectra displayed in Fig.3(a) and Fig.4(a) were recorded. Cyan lines in (b) indicate the direction of the 2H-axis (see text) of the molecules. (d,e) Top views of the DFT calculated relaxed most stable adsorption geometries.

In C-phase, (Fig. 2(b)), the splitting of the two lobes that are perpendicular to the 2H-axis is used as well as a convenient topographic feature to determine the angle δ, defined relative to the close-packed directions of Ag(111) as sketched. The measured value of δ is $65° \pm 3°$ similar within the angle error to the azimuthal orientation of the most stable adsorption configuration α. The structural model of the molecules self-organized as a C-phase obtained by DFT calculations is shown in Fig.2(c). The angle $\delta = 62°$ is in excellent agreement with the experimental value validitating this model to further extract the projected density of states (PDOS). The extra insight we get from this STM analysis is that molecules in the less stable configuration such as molecule C in Fig.1 (b) undergo an azimuthal rotation of about 30° upon self-assembling. Therefore, one expects the ratio between the two configurations to increase when increasing the coverage in favor of α configuration. However, this analysis is out of the range of this paper.

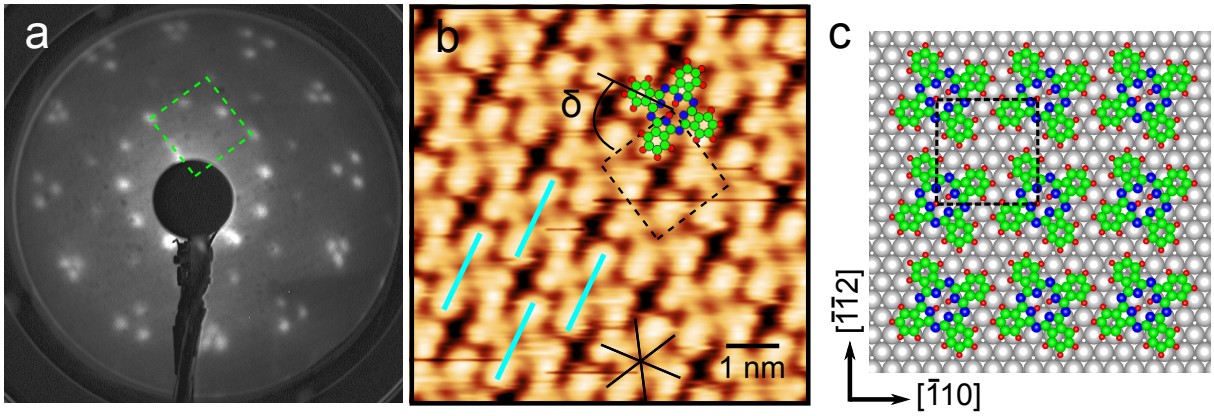

Figure 2: **The Structure of 2HPc/Ag(111) in C-phase.** (a) LEED pattern recorded at an electron energy of 14 eV. (b) Corresponding STM topographic image. Tunneling bias conditions: $V_b = -1.8$ V, $I_t = 200$ pA. The close-packed $\langle 01\bar{1} \rangle$ directions of the Ag(111) are indicated by the black star. Cyan lines indicate the direction of the 2H-axis of the molecules (see text). (c) Top view of the simulated relaxed adsorption geometry. Rectangles in dashed line represent the unit cells in (a) reciprocal and (b,c) direct space.

IV-ELECTRONIC STRUCTURE

IV-a: Kondo effect in single molecules

In previous works, it was demonstrated from UPS and two-photon photoemission (TPPE) measurements that charge transfer occurs from the Ag susbtrate to the Pc ligand of 2HPc.[38,39] In the C-phase, this was evidenced by the occupancy of the LUMO orbital upon adsorption resulting in a state located at an energy of $-0.15\,\mathrm{eV}$ and that was called former-LUMO (F-LUMO) in reference to the LUMO state of the free molecule. In addition, an unoccupied HIS is formed, resulting from the hybridization of the Shockley surface state of Ag(111) with the first LUMO state of the free 2HPc molecule. This nearly-free electron state was characterized by a band onset located at an energy of $+0.23 \pm 0.03\,\mathrm{eV}$ above $\mathrm{E_F}$. Knowing the abovementioned results, one can reasonably raise the following question: would self-assembled 2HPc behave like 1/2-spin in contact with a free electron bath possibly giving rise to Kondo effect? Would this effect persists for single molecules? To elucidate the arising of a Kondo effect for a single molecule as well as for a self-assembly, we performed STS and UPS on G and C-phases.

First, we address the Kondo effect in single molecules using STS and UPS. STS spectra in the enery range around $\mathrm{E_F}$ are reported in Fig.3(a). They were recorded with the STM tip located above molecules A, B and C displayed in Fig.1(c). All tunneling spectra show two main characteristics: (i) a sharp electronic resonance in the close vicinity of $\mathrm{E_F}$, labeled κ in Fig.3(a), (ii) a conductance peak located at about $+52\,\mathrm{meV}$, labeled ν. As no molecular nor substrate's state is expected in a range of $\pm 10\,\mathrm{meV}$ around $\mathrm{E_F}$, we can, as a first guess, reasonably attribute the resonance at $\mathrm{E_F}$ to Kondo effect. Yet, as other phenomena could lead to the formation of a peak in the differential conductance spectrum next to $\mathrm{E_F}$, a magnetic field or temperature dependency of the full width at half maximum (FWHM) of the resonance should be recorded and compared to laws governing the effect in order to unambiguously attribute its origin to Kondo effect.[87,88] Alternatively, UPS can be used

since a typical spectrum of a Kondo system exhibits a sharp resonance at E_F at temperatures below the Kondo temperature T_K.[87,89,90] Upon increasing temperature, this peak is expected to broaden and decrease in intensity.[91–93] Such relationships with temperature is what is experimentally observed as displayed in Fig. 3(b) showing UPS spectra recorded at temperatures of 9 K, 80 K and 285 K. At T= 9 K, a narrow and intense peak is observed at E_F. At T= 80 K, the peak is larger and its intensity is strongly reduced to finally almost vanish at T= 285 K. This effect of the temperature is emphasized using the normalization by the Fermi-Dirac function as shown in the inset of Fig.3(b).

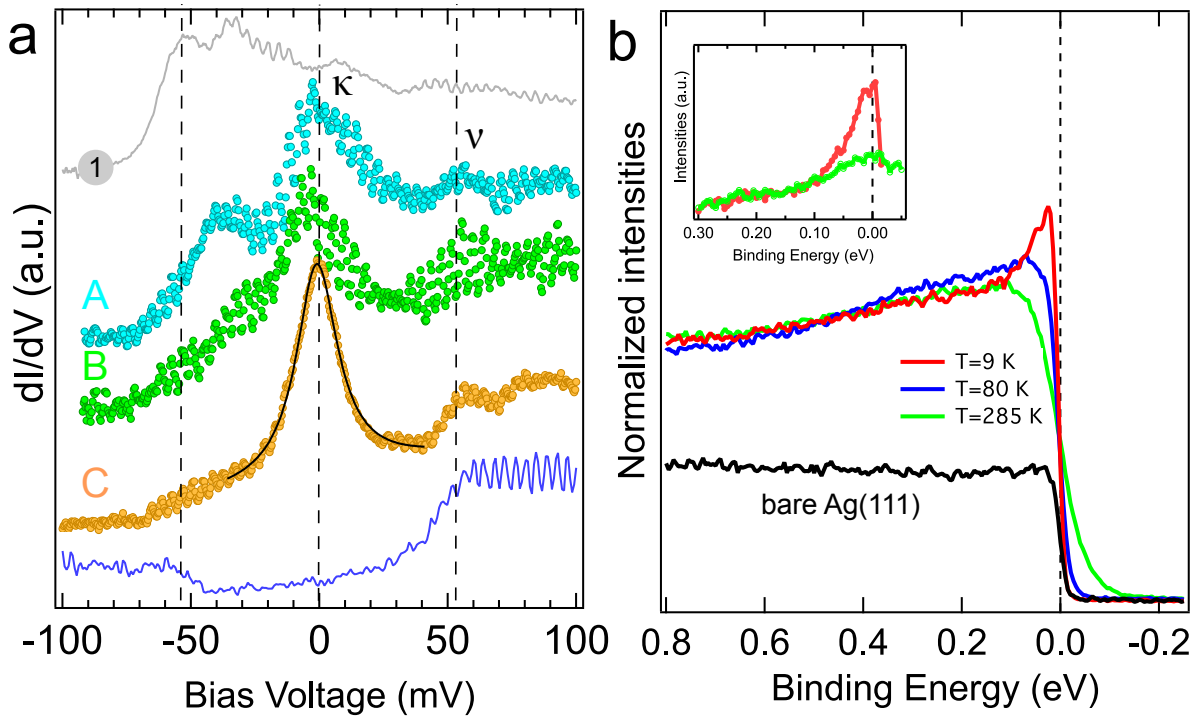

Figure 3: **Electronic properties of 2HPc/Ag(111) in G-phase** (a) Dotted lines are dI/dV spectra recorded above molecules labeled A,B and C in Fig.1(c). The full grey line was recorded further away from the molecules on bare Ag surface at the position indicated by the grey cross in Fig. 1(c). Set points are: $V_b = 1\,mV$, $I_t = 200\,pA$ and $V_b = 25\,mV$, $I_t = 200\,pA$ for bottom curve. The Fano fit represented by the black line superimposed to the orange curve yields: $q = 54$, $\epsilon_K = -1.16\,meV$ and $\Gamma = 9.8$. A vertical shift was added for clarity. (b) UPS spectra recorded at T= 9 K, 80 K and 285 K and on bare Ag(111) substrate at T= 9 K (black line) and at an emission angle of 45°. The inset are the corresponding UPS spectra divided by the Fermi-Dirac function.

The resonance observed in UPS spectra can not be assigned to any state of the sub-

strate since the UPS spectrum recorded under the same experimental conditions on the bare Ag(111) surface is flat next to E_F as shown as the black line in Fig.3(b). Thanks to the concomitance of a resonance at E_F in the STS spectrum and the temperature behavior of the photoemission feature at E_F , one can now unambiguously attribute it to a Kondo resonance.

According to Refs.,[32,33] T_K can be roughly determined by fitting the Kondo resonance with a Fano function lineshape expressed as, disregarding the instrumental broadening:[94,95]

$$\frac{(q+\epsilon)^2}{(1+\epsilon^2)};\ \ \epsilon = \frac{eV-\epsilon_k}{\Gamma} \tag{1}$$

with Γ the 1/2 FWHM such that $\Gamma = k_B T_K$.

The mean fitted T_K value obtained on molecule C is $T_K = 108 \pm 6\,K$ with $q >> 1$. As an example, the fitting result of the dI/dV spectrum recorded at the center of molecule C is shown in Fig. 3(a) as a black line. The high q values indicates that the tunneling process occurs preferentially through the molecular orbital than to the conduction-electron continuum.

The next feature of the STS spectra to be discussed is the peak ν at $E_\nu = 52 \pm 5\,meV$. This side feature appears as a resonance and its intensity with respect to the zero-bias one varies depends on the tip location. At tunneling parameters for which the Kondo resonance is not observed, the dI/dV spectrum has an upside down hat shape as depicted in Fig.3(a). The two step-edges are located at about $\pm E_\nu$ which is the standard lineshape observed when inelastic processes corresponding to vibrational excitation energies of E_ν get activated. However, the side feature appears more as a resonance than as a step. According to,[96–100] it can be understood as originating from the splitting of the zero-bias resonance resulting

from the electron-vibron coupling. Other Kondo organic/inorganic systems exhibit as well, such peaks of vibronic nature.[28,29,40,101,102] In particular, conductance spectra recorded over CuPc and NiPc on Ag(100) exhibit such fingerprints at comparable excitation energies[28,29] and might correspond to the activation of torsion modes.[103]

IV-b: Electronic surface properties of Ag(111)

To utterly describe the organometallic interface, the Ag properties must be investigated as well. Moreover, their knowledge will help us better understand the Kondo effect. In the following, we are interested in the modifications of the Ag surface properties when a very small amount of molecules is adsorbed such as in Fig. 1(b). To begin with, we have recorded a dI/dV curve on pristine Ag(111) prior to molecular adsorption. It is shown as a green curve in Fig.4(a). Its lineshape and energy onset is typical of the well-known Ag Shockley surface state.[68,104,105] After molecular adsorption at low coverage, a dI/dV spectra have been recorded on the uncovered Ag surface in between molecules. They are quite different compared to the one observed on the pristine Ag surface and they depend strongly on the location where they were recorded. Spectra 2 to 4 are given in Fig.4(a) as examples. The spectra can be described as a step-like lineshape with prominent peaks superimposed to it. As will be explained below, those extra peaks are eigenstates resulting from electron confinement. STM and conductance maps are shown in Fig.4(b-f). A strong spatially textured background between the molecules is observed for energies eV_b above the Ag Shockley state energy onset E_0. This is illustrated by the STM image recorded at $-40\,\mathrm{meV}$ in Fig.4(b). The effect is even better evidenced on the three conductance maps shown in Fig.4(c-f). Indeed, whereas the dI/dV map recorded at $-0.1\,\mathrm{V}$ in (c) shows a constant and homogeneous background, strong variation of the conductance is observed on the flat areas of bare Ag between the molecules for the map above for $eV_b > E_0$ in Fig.4(d-f). Moreover, it depends strongly on the energy. Due to these characteristics, we attribute these observations to the formation of standing wave patterns resulting from the scattering of the 2D nearly free electron sur-

face state of Ag. In other words, 2HPc molecules act as electron scatterers of nanometric size.

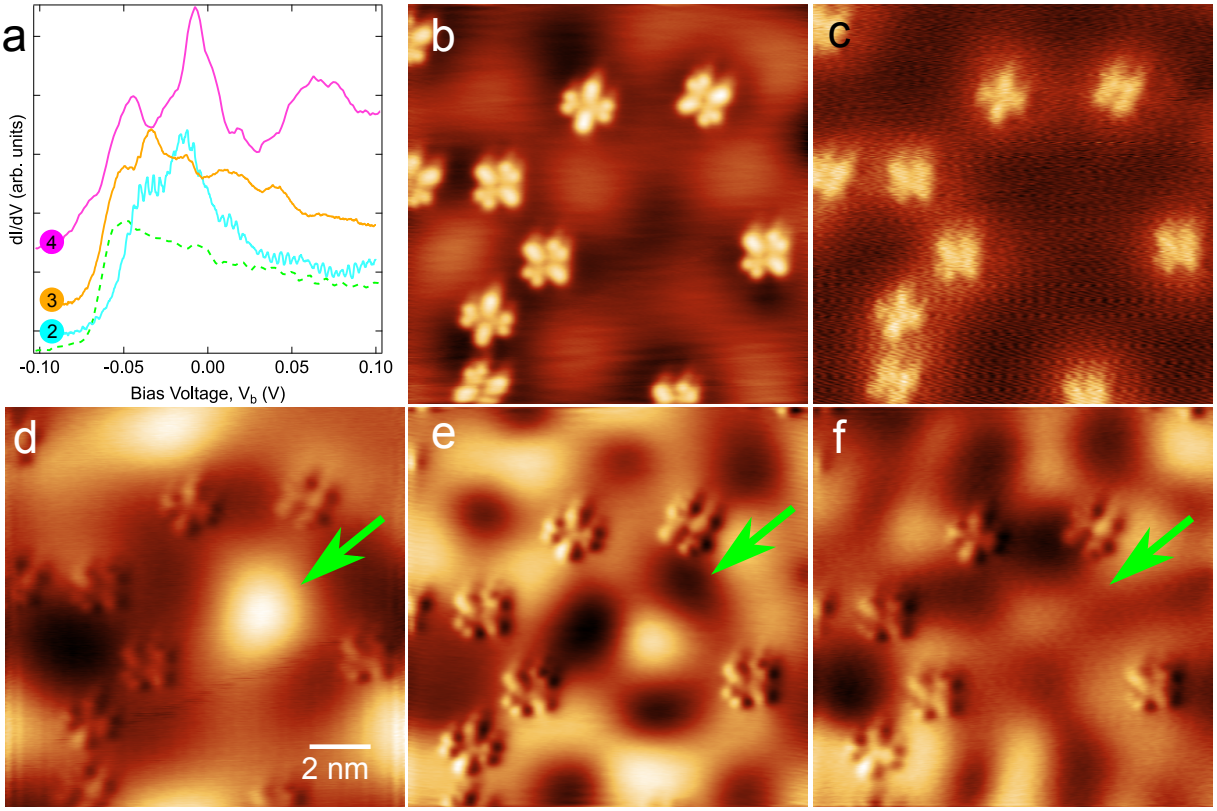

Figure 4: **Electronic properties of Ag in G-phase**. (a) dI/dV spectra recorded on Ag(111) between molecules in solid lines and on a pristine Ag(111) surface in dashed line. Numerical labels 2 to 4 correspond to the position of the tip marked by a matching colored cross in Fig.1(c) and Fig.7(b). Tunneling bias conditions: $V_b = -1.8\,V$, $I_t = 200\,pA$. (b) STM topographic image. Tunneling bias conditions: $V_b = -40\,mV$, $I_t = 200\,pA$,(c-f) dI/dV maps recorded at $-100\,mV$,$-40\,mV$,$+10\,mV$ and $+30\,mV$, respectively. Tunneling current $I_t = 200\,pA$.

On those maps, the most surprising feature is the one observed at the center of the image as pointed by the green arrow in Fig.4(d-f) that is reminiscent of electron confinement in closed 2D artificial hexagonal Ag nanovacancies,[106] nanoislands[107–109] or even 2D porous molecular networks adsorbed on coinage (111) metal surfaces.[110] What is remarkable is that, contrary to those 2D resonators that are closed structures delimited by hard walls, the pattern of this current work have been obtained with only 4 to 5 molecules that are

2 to 5 nm apart and thus forming an open structure. In the abovementioned examples of electron confinement, the potential barrier is considered as continuous whereas it is obviously discontinuous in the present work. Shchyrba *et al.* showed previously partial confinement insides molecular pores with missing borders.[111] Pennec *et al.* showed confinement of the Ag surface state in a U-shaped cavity formed of linear molecular walls. However, to the best of our knowledge, the formation of an open walls molecular confining cavity has not been evidenced yet and therefore deserve a keen interest.

Scattering of the surface state of (111) surfaces of coinage metals by π- conjugated molecules have been previously observed.[112–116] When self-assembled in specific ways such as in Ref.[115] or organized in metal-organic frameworks, molecules can act as scattering walls for electrons of a two-dimensional electron gas. Quantum well arrays can thus be formed with well-defined molecular boundaries. Single π-conjugated molecular scatterer has been modeled[112] as a collection of atomic total absorbers at the position of the carbon atoms using multiple scattering expansion as developped for quantum corrals.[117] In molecular porous networks, scattering molecules are described in the framework of the boundary elements method where molecular boundaries correspond to constant rectangular potential.[114] The case of 2HPc on Ag(111) at low coverage is singular in the sense that it represents an intermediate case between the two situations cited above. Therefore, to explain the patterns observed in our work, a complementary theoretical approach might be necessary and further experimental investigations are required. This demonstrates that the 2HPc/Ag(111) interface offers the possibility to explore new fundamental aspects of quantum physics *i.e.* the electron scattering by an object of nanometric size composed of a collection of atomic-like scatterers covalently bonded. Besides, it holds promise for the design of tunable low-dimensional electron resonator. As will be discussed in section V, quantum confinement might have a non negligible impact on the Kondo effect.

IV-c: Kondo effect in self-assembly

To investigate the arising of a Kondo effect in the commensurate C-phase self-assembly, STS and UPS were carried out. Results are displayed in Fig.5. To start with, STS was recorded over a large bias voltage range to investigate the overall electronic properties of the interface. Whereas UPS probe occupied states only, STS gives access to energy regions above and below Fermi level in a single-shot experiment enabling a direct comparison with UPS and TPPE spectra of previous studies.[38,39] The differential conductance dI/dV spectrum in Fig.5(a) reveals distinct peaks that can unambiguously be assigned. Peaks located at about $-0.12\,\mathrm{V}$ and $-1.2\,\mathrm{V}$ are attributed to F-LUMO and HOMO, respectively according to ref.[38,118] At positive bias, the step-like feature which is typical of a nearly-free electron two-dimensional gas is assigned to the HIS. Its edge is located at $+0.23 \pm 0.01\,\mathrm{V}$, in very good agreement with the band edge measured by TPPE.[39] The F-LUMO and HOMO states are also detected by UPS as indicated in Fig.8 in the Supporting Information. As already explained in ref.,[38] the presence of an occupied F-LUMO state results from the charge transfer from the Ag surface to the molecule. Hence, both our STS and UPS experiments show that the molecule is negatively charged in agreement with these previous results. As well as for single molecules, a resonance at $\mathrm{E_F}$ was obtained using STS and UPS techniques. Bringing forward the same arguments as for the case of single molecules, one can conclude that this resonance can be ascribed to a Kondo effect. A high-resolution STS spectrum in Fig.5(b) exhibits as in the case of single 2HPc, an extra peak at about 50 meV leading to the conclusion that electron-vibron coupling is not hindered by intermolecular interactions inside the self-assembly thus resulting in a vibrational Kondo effect. Once again, this is corroborated by the inelastic electron tunneling spectrum shown in blue line in Fig.5(b) recorded over the Pc ligand and exhibiting the characteristic symmetric two-step like lineshape. The Kondo temperature $\mathrm{T_K}$ obtained by fitting the STS spectra recorded over 10 molecules inside the supramolecular network ranges from 57 to 69 K. It is about twice smaller than for single molecules. Possible explanations for the difference between the two phases will be discussed in section V .

IV-d: Density of states calculated by DFT

In order to correlate spectroscopic peaks observed in STS and UPS spectra with the molecular electronic structure, we have computed the DOS of 2HPc in C-phase and projected it onto atomic orbitals. As shown in Fig.5(d), this PDOS is dominated by orbitals of p_z character. One peak below -1 eV corresponds to the HOMO state of the molecule. Crossing E_F, another prominent peak of p_z character corresponds to the F-LUMO state. Although the calculated energy position of this state is upshifted compared to experiments due to a well-known drawback of standard DFT calculations that do not properly account for HOMO-LUMO gap, it remains in good agreement with experimental data and supports the identification of the electronic states of the dI/dV spectrum of Fig.5(a).

A net charge transfer of $0.32e^-$ from the substrate to the adsorbate region occurs. Again, this value is only qualitative since charge transfer estimated from DFT calculations depends critically on the computational details.[119] Spin density distributions have been calculated as well and are shown in Fig.5(e). Obviously, the no spin bearing free 2HPc molecule does not exhibit any spin density (Fig.5(e),left). However, upon adsorption on Ag(111), (Fig.5(e),right) we observe a distribution of the spin electron density in the inner region of the molecule situated mostly on the pyrrole parts. This is very similar to what is observed for the anionic species as displayed in Fig.5(e) (center panel). The DFT results confirm the scenario that the origin of the Kondo effect can be attributed to the partial filling of the π states of the molecule occuring upon adsorption on the silver surface.

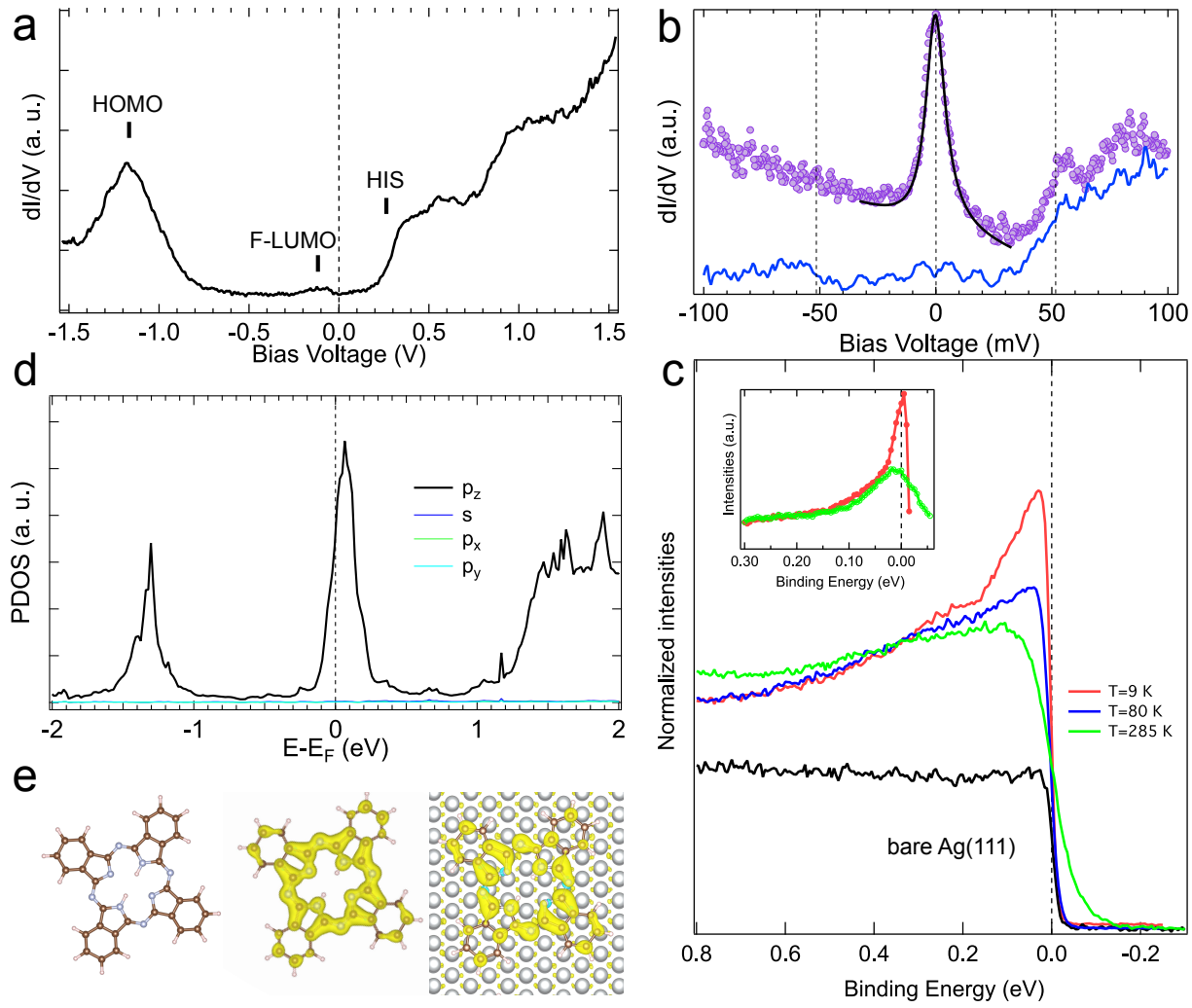

Figure 5: **Electronic properties of 2HPc/Ag(111) in C-phase.** (a,b) dI/dV spectra recorded over the center of one molecule in the self-assembly. Set point are (a) $V_b = -1\,V$, $I_t = 100\,pA$, (b) $V_b = 1\,mV$, $I_t = 200\,pA$ for top curve and $V_b = 50\,mV$, $I_t = 200\,pA$ for bottom curve. A vertical shift was added for clarity. The Fano fit represented by the black line superimposed to the top curve in (b) yields: $q = 21$, $\epsilon_K = -0.35\,meV$ and $\Gamma = 5.0$. (c) UPS spectra recorded at T= 9 K, 80 K, 285 K and on bare Ag(111) substrate at T= 9 K at an emission angle of 45°. The inset are the corresponding UPS spectra divided by the Fermi-Dirac function. (d) Computed density of states projected (PDOS) onto atomic orbitals of 2HPc on Ag(111) assembled in phase C, (e) from left to right: spin density distribution of neutral, anionic 2HPc species in the gas-phase and adsorbed on Ag(111). The sign of the spin is indicated in yellow/cyan. The isovalue for the electronic spin density is roughly 10^{-7} e/Å^3 in both cases.

V-DISCUSSION

In this section, we would like to address the mechanism behind the variation of T_K with the molecular density. In previous sections, we have shown that T_K is about twice smaller in the C-phase compared to the G-phase.

A first possible explanation could lie in the effect of intermolecular interactions. It has been shown in some Pc supramolecular assemblies that ligand-ligand interaction could engender a lifting of the molecules, reducing the molecule-substrate coupling and thus, T_K .[28,56] However, according to our DFT calculations, the adsorption height varies only minutely between the two phases. In addition, as shown in Fig.9 in the Supporting Information, the PDOS of the 2HPc molecule on Ag(111) at low concentration is very similar to the one of molecules in the C-phase reported in Fig.5(d). The position of the F-LUMO varies only a little and a charge transfer of 0.27 electrons has been extracted. This is very close to the value of 0.32 electrons obtained for the self-assembly. This supposes that the coupling strength with the substrate doesn't vary much upon formation of the C-phase and can not account for the strong variation of T_K .

The Ruderman-Kittel-Kasuya-Yoshida (RKKY) interaction is an alternative origin. It is an indirect spin-spin interaction mediated by the conduction electrons of the metal. Depending on distance, it favours ferromagnetic or antiferromagnetic (AFM) alignments of magnetic moments. It has been shown that an interplay between the Kondo effect and the RKKY interaction exists in supramolecular assemblies.[52,62] The width of the Abrikosov-Suhl resonance is strongly affected or even suppressed due to the magnetic coupling between the spins. More specifically, FM RKKY interaction sharpens the resonance and, on the other hand, the AFM RKKY broadens it.[120] Unfortunately, it is very challenging to test the assumption whether RKKY interaction is responsible for the reduction of T_K in the self-assembly. Indeed, in order to demonstrate it, a thought experiment would be to measure T_K by STS as a

function of the molecule-molecule distance for a pair of molecules to mimic the conditions of the two-impurities Kondo problem.[121] However, in such a case of a molecular pair, surface electrons would dominate the RKKY interaction due to their lower k_F compared to bulk electrons and couldn't be used to conclude on the exchange coupling in the self-assembly for which the surface state has hybridized with a molecular orbital to form the unoccupied HIS. Nevertheless, one can tentitatively apply the following formula to predict the sign of the exchange coupling in the commensurate phase: $J = J_0 \frac{sin(2k_F r)}{(2k_F r)^2}$, where k_F is the Fermi wave vector of the substrate and r, the distance between the spins. We use the lattice parameters extracted from our DFT calculations (1.51 nm and 1.45 nm) and $k_F = 12.02\,nm^{-1}$.[122] Moreover, we discard the influence of the second-nearest neighbors due to the fast decay of the exchange for bulk electrons. The result gives an AFM coupling between nearest-neighbors molecules. This would lead to an increase of T_K compared with the single impurity case which contradicts our experimental findings. Therefore RKKY can not account for the decrease of T_K upon formation of self-assembly.

The observed variation of T_K could be alternatively explained considering that T_K is directly proportional to $\exp^{\frac{-1}{\rho_F J}}$,[87] where ρ_F is the substrate's density of states at the Fermi energy and J is the exchange coupling at the magnetic impurity.[87] This relationship indicates that when ρ_F is reduced, T_K is reduced as a result. At low molecular concentration, the uncovered substrate exhibits a Shockley surface state that participates to ρ_F. In the case of the C-phase, as this state hybridizes with the LUMO state of the free molecule to form the HIS shifted above E_F , ρ_F is reduced in comparison with the isolated molecules and thus, would explain the decrease of T_K for the C-phase.

The influence of the surface state on the Kondo resonance width has been a topic of debate for many years (see Ref.[123] and references therein). Some works on Ag(111) have suggested a minor role for surface-state electrons in the Kondo effect.[124] Only very recently,

Li et al. tackle this controversy using LT-STM/STS on Co adsorbates on Ag(111).[123] They unambiguously demonstrate the influence of the surface state on the Kondo resonance by measuring the width of the zero-bias peak as a function of the lateral distance to the impurity. The key point is that they evidenced an oscillatory dependency as a function of the distance to the magnetic impurity which periodicity matches the half Fermi wavelength of the Ag(111) surface state. Moro-Lagares *et al.* obtained experimentally and theoretically a nearly linear relationship between T_K and the surface-state contribution local density of states of the substrate.[125] Besides, both works emphasize the effect of quantum confinement of the surface state. In particular, it was evidenced that in a quantum corral, the Kondo width can be significantly increased (more than three times).[123] As, at low molecular density in the 2HPc/Ag(111) system, quantum confinement of the Ag surface state is also observed, it probably also plays a significant role on the high value of T_K in G-phases. The effect of the Shockley surface state on T_K has also been observed on molecules such as Co-tetraphenylporphirin on Cu(111).[113] In this work, Iancu *et al.* showed that molecules exposed to Cu surface state electrons exhibit a higher T_K than molecules inside a self-assembled cluster. These results are in favor of our interpretation.

VI-CONCLUSIONS

As a conclusion, we have studied the electronic properties of the metal-free phthalocyanine 2HPc adsorbed on Ag(111) surfaces by means of scanning tunneling and photoelectron spectroscopies and compared the experimental results with DFT calculations. We have evidenced a partial filling of a molecular π state lying next to the Fermi level. The presence of this extra π-spin in the molecule leads to the emergence of a Kondo effect at low temperature for single molecules as well as for molecules arranged in a 2D self-assembly. We have demonstrated the strong influence of the surface electronic properties of the substrate on the Kondo temperature.

The fact that we deal with a metal-free phthalocyanine offer many future prospects. In other words, the absence of a metal ion at the center of the molecule is the asset of this system. Indeed, it has been shown that this metal free central cavity of 2HPc can be manipulated by STM in many ways: tautomerization[84], partial or total deshydrogenation or direct Ag metalation can be induced.[46] Therefore, one can envisage to investigate the influence of such modifications on the Kondo physics. As an example, a 2HPc molecule can be transformed into an AgPc molecule in the self-assembly[46] and study the effect on T_K. In that case, T_K is likely to change through the modification of the local coupling with the substrate via the up or down-lifting of the molecules or the RKKY interaction between neighbouring molecules.

Besides the STM manipulation-based approach, local modification of the electronic and magnetic properties of 2HPc can be obtained by on- surface synthesis such as chemical doping or metallation upon adsorption of alkali or metallic atoms under UHV.[26,85] Using Li dopants, the charge transfer could be locally modulated and the molecular spin could be tuned[26]. In another study, Bai *et al.* showed that 2HPc react strongly with Fe atoms to form FePc molecules on Ag(111).[85] This on-surface metalation process was theoretically shown to be energetically favorable for M=Co, Ni, Mn on 2HPc/Ag(111).[126] It would be particularly interesting to study the Kondo physics in the MPc/2HPc hetero-molecular arrays as a function of MPc concentration. Overall, any combination of the above cited manipulation strategies might be used. For these reasons, this system offers an exceptionnaly rich playground for investigating the molecular Kondo physics.

References

1. Urtizberea, A.; Natividad, E.; Alonso, P. J.; Andrés, M. A.; Gascón, I.; Goldmann, M.; Roubeau, O. Advanced Functional Materials 2018, 28, 1801695–15.

2. Gaita-Ariño, A.; Luis, F.; Hill, S.; Coronado, E. Nature Chemistry 2019, 11, 301–309.

3. Cavallini, M.; Gomez-Segura, J.; Ruiz-Molina, D.; Massi, M.; Albonetti, C.; Rovira, C.; Veciana, J.; Biscarini, F. Angewandte Chemie International Edition 2005, 44, 888–892.

4. Cinchetti, M.; Dediu, V. A.; Hueso, L. E. Nature Materials 2017, 16, 507–515.

5. Bogani, L.; Wernsdorfer, W. Nature Materials 2008, 7, 179–186.

6. Mannini, M.; Pineider, F.; Sainctavit, P.; Danieli, C.; Otero, E.; Sciancalepore, C.; Talarico, A. M.; Arrio, M.-A.; Cornia, A.; Gatteschi, D. et al. Nature Materials 2009, 8, 194–197.

7. Guo, F.-S.; Day, B. M.; Chen, Y.-C.; Tong, M.-L.; Mansikkamäki, A.; Layfield, R. A. Angewandte Chemie International Edition 2017, 56, 11445–11449.

8. Zhao, A. Science 2005, 309, 1542–1544.

9. Li, Z.; Li, B.; Yang, J.; Hou, J. G. Accounts of Chemical Research 2010, 43, 954–962.

10. Niu, T.; Li, A. The Journal of Physical Chemistry Letters 2013, 4, 4095–4102.

11. Komeda, T.; Katoh, K.; Yamashita, M. Progress in Surface Science 2014, 89, 127–160.

12. Ishikawa, N.; Sugita, M.; Ishikawa, T.; ya Koshihara, S.; Kaizu, Y. Journal of the American Chemical Society 2003, 125, 8694–8695.

13. Ishikawa, N.; Sugita, M.; Wernsdorfer, W. Angewandte Chemie International Edition 2005, 44, 2931–2935.

14. Urdampilleta, M.; Klyatskaya, S.; Cleuziou, J.-P.; Ruben, M.; Wernsdorfer, W. Nature Materials 2011, 10, 502–506.

15. Gottfried, J. M. Surface Science Reports 2015, 70, 259–379.

16. Amsterdam, S. H.; Stanev, T. K.; Zhou, Q.; Lou, A. J. T.; Bergeron, H.; Darancet, P.; Hersam, M. C.; Stern, N. P.; Marks, T. J. ACS Nano 2019, 13, 4183–4190.

17. Kafle, T. R.; Kattel, B.; Lane, S. D.; Wang, T.; Zhao, H.; Chan, W.-L. ACS Nano 2017, 11, 10184–10192.

18. Padgaonkar, S.; Amsterdam, S. H.; Bergeron, H.; Su, K.; Marks, T. J.; Hersam, M. C.; Weiss, E. A. The Journal of Physical Chemistry C 2019, 123, 13337–13343.

19. Suzuki, T.; Kurahashi, M.; Ju, X.; Yamauchi, Y. The Journal of Physical Chemistry B 2002, 106, 11553–11556.

20. Atodiresei, N.; Brede, J.; Lazić, P.; Caciuc, V.; Hoffmann, G.; Wiesendanger, R.; Blügel, S. Physical Review Letters 2010, 105, 066601.

21. Djeghloul, F.; Gruber, M.; Urbain, E.; Xenioti, D.; Joly, L.; Boukari, S.; Arabski, J.; Bulou, H.; Scheurer, F.; Bertran, F. et al. The Journal of Physical Chemistry Letters 2016, 7, 2310–2315.

22. Delprat, S.; Galbiati, M.; Tatay, S.; Quinard, B.; Barraud, C.; Petroff, F.; Seneor, P.; Mattana, R. Journal of Physics D: Applied Physics 2018, 51.

23. Caputo, M.; Panighel, M.; Lisi, S.; Khalil, L.; Santo, G. D.; Papalazarou, E.; Hruban, A.; Konczykowski, M.; Krusin-Elbaum, L.; Aliev, Z. S. et al. Nano Letters 2016, 16, 3409–3414.

24. Bauer, J.; Pascual, J. I.; Franke, K. J. Physical Review B 2013, 87, 075125.

25. Malavolti, L.; Briganti, M.; Hänze, M.; Serrano, G.; Cimatti, I.; McMurtrie, G.; Otero, E.; Ohresser, P.; Totti, F.; Mannini, M. et al. Nano Letters 2018, 18, 7955–7961.

26. Krull, C.; Robles, R.; Mugarza, A.; Gambardella, P. Nature Materials 2013, 12, 337–343.

27. Ballav, N.; Wäckerlin, C.; Siewert, D.; Oppeneer, P. M.; Jung, T. A. The Journal of Physical Chemistry Letters 2013, 4, 2303–2311.

28. Mugarza, A.; Krull, C.; Robles, R.; Stepanow, S.; Ceballos, G.; Gambardella, P. Nature Communications 2011, 2, 490.

29. Mugarza, A.; Robles, R.; Krull, C.; Korytár, R.; Lorente, N.; Gambardella, P. Physical Review B 2012, 85, 155437–13.

30. Anderson, P. W. Physical Review 1961, 124, 41–53.

31. Kondo, J. Progress of Theoretical Physics 1964, 32, 37–49.

32. Li, J.; Schneider, W.-D.; Berndt, R.; Delley, B. Physical Review Letters 1998, 80, 2893–2896.

33. Madhavan, V.; Chen, W.; Jamneala, T.; Crommie, M. F.; Wingreen, N. S. Science 1998, 280, 567–569.

34. Komeda, T. Surface Science 2014, 630, 343–355.

35. Ternes, M.; Heinrich, A. J.; Schneider, W.-D. Journal of Physics: Condensed Matter 2008, 21, 053001.

36. Toader, M.; Shukrynau, P.; Knupfer, M.; Zahn, D. R. T.; Hietschold, M. Langmuir 2012, 28, 13325–13330.

37. Gorgoi, M.; Zahn, D. R. Applied Surface Science 2006, 252, 5453–5456.

38. Kröger, I.; Bayersdorfer, P.; Stadtmüller, B.; Kleimann, C.; Mercurio, G.; Reinert, F.; Kumpf, C. Physical Review B 2012, 86, 195412.

39. Caplins, B. W.; Suich, D. E.; Shearer, A. J.; Harris, C. B. The Journal of Physical Chemistry Letters 2014, 5, 1679–1684.

40. Fernández-Torrente, I.; Franke, K. J.; Pascual, J. I. Physical Review Letters 2008, 101, 217203.

41. Choi, T.; Bedwani, S.; Rochefort, A.; Chen, C.-Y.; Epstein, A. J.; Gupta, J. A. Nano Letters 2010, 10, 4175–4180.

42. Liu, J.; Isshiki, H.; Katoh, K.; Morita, T.; Brian, K. B.; Yamashita, M.; Komeda, T. Journal of the American Chemical Society 2012, 135, 651–658.

43. Requist, R.; Modesti, S.; Baruselli, P. P.; Smogunov, A.; Fabrizio, M.; Tosatti, E. Proceedings of the National Academy of Sciences 2013, 111, 69–74.

44. Esat, T.; Lechtenberg, B.; Deilmann, T.; Wagner, C.; Krüger, P.; Temirov, R.; Rohlfing, M.; Anders, F. B.; Tautz, F. S. Nature Physics 2016, 12, 867–873.

45. Karan, S.; Li, N.; Zhang, Y.; He, Y.; Hong, I.-P.; Song, H.; Lü, J.-T.; Wang, Y.; Peng, L.; Wu, K. et al. Physical Review Letters 2016, 116, 027201.

46. Sperl, A.; Kröger, J.; Berndt, R. Angewandte Chemie International Edition 2011, 50, 5294–5297.

47. Perera, U. G. E.; Kulik, H. J.; Iancu, V.; da Silva, L. G. G. V. D.; Ulloa, S. E.; Marzari, N.; Hla, S.-W. Physical Review Letters 2010, 105, 106601.

48. Booth, C. H.; Walter, M. D.; Daniel, M.; Lukens, W. W.; Andersen, R. A. Physical Review Letters 2005, 95, 267202.

49. Wahl, P.; Diekhöner, L.; Wittich, G.; Vitali, L.; Schneider, M. A.; Kern, K. Physical Review Letters 2005, 95, 166601.

50. Zhao, A.; Hu, Z.; Wang, B.; Xiao, X.; Yang, J.; Hou, J. G. The Journal of Chemical Physics 2008, 128, 234705.

51. Scott, G. D.; Natelson, D. ACS Nano 2010, 4, 3560–3579.

52. Tsukahara, N.; Shiraki, S.; Itou, S.; Ohta, N.; Takagi, N.; Kawai, M. Physical Review Letters 2011, 106, 187201.

53. Minamitani, E.; Tsukahara, N.; Matsunaka, D.; Kim, Y.; Takagi, N.; Kawai, M. Physical Review Letters 2012, 109, 086602.

54. Ziroff, J.; Hame, S.; Kochler, M.; Bendounan, A.; Schöll, A.; Reinert, F. Physical Review B 2012, 85, 161404.

55. Garnica, M.; Stradi, D.; Barja, S.; Calleja, F.; Díaz, C.; Alcamí, M.; Martín, N.; de Parga, A. L. V.; Martín, F.; Miranda, R. Nature Physics 2013, 9, 368–374.

56. Komeda, T.; Isshiki, H.; Liu, J.; Katoh, K.; Shirakata, M.; Breedlove, B. K.; Yamashita, M. ACS Nano 2013, 7, 1092–1099.

57. Iancu, V.; Braun, K.-F.; Schouteden, K.; Haesendonck, C. V. Physical Review Letters 2014, 113, 106102.

58. Lin, T.; Kuang, G.; Wang, W.; Lin, N. ACS Nano 2014, 8, 8310–8316.

59. Zhang, Q.; Kuang, G.; Pang, R.; Shi, X.; Lin, N. ACS Nano 2015, 9, 12521–12528.

60. Maughan, B.; Zahl, P.; Sutter, P.; Monti, O. L. A. The Journal of Physical Chemistry Letters 2017, 8, 1837–1844.

61. Hiraoka, R.; Minamitani, E.; Arafune, R.; Tsukahara, N.; Watanabe, S.; Kawai, M.; Takagi, N. Nature Communications 2017, 8, 1–7.

62. Tuerhong, R.; Ngassam, F.; Watanabe, S.; Onoe, J.; Alouani, M.; Bucher, J.-P. The Journal of Physical Chemistry C 2018, 122, 20046–20054.

63. Temirov, R.; Soubatch, S.; Luican, A.; Tautz, F. S. Nature 2006, 444, 350–353.

64. Armbrust, N.; Schiller, F.; Güdde, J.; Höfer, U. Scientific Reports 2017, 7, 1–8.

65. Lerch, A.; Fernandez, L.; Ilyn, M.; Gastaldo, M.; Paradinas, M.; Valbuena, M. A.; Mugarza, A.; Ibrahim, A. B. M.; Sundermeyer, J.; Höfer, U. et al. The Journal of Physical Chemistry C 2017, 121, 25353–25363.

66. Gerbert, D.; Hofmann, O. T.; Tegeder, P. The Journal of Physical Chemistry C 2018, 122, 27554–27560.

67. Sabitova, A.; Temirov, R.; Tautz, F. S. Physical Review B 2018, 98, 205429.

68. Bürgi, L.; Knorr, N.; Brune, H.; Schneider, M.; Kern, K. Applied Physics A: Materials Science & Processing 2002, 75, 141–145.

69. Reinert, F.; Nicolay, G.; Schmidt, S.; Ehm, D.; Hüfner, S. Physical Review B 2001, 63, 115415.

70. Puschnig, P.; Berkebile, S.; Fleming, A. J.; Koller, G.; Emtsev, K.; Seyller, T.; Riley, J. D.; Ambrosch-Draxl, C.; Netzer, F. P.; Ramsey, M. G. Science 2009, 326, 702–706.

71. Gargiani, P.; Betti, M. G.; Taleb-Ibrahimi, A.; Le Fèvre, P.; Modesti, S. The Journal of Physical Chemistry C 2016, 117, 26144–26155.

72. Kresse, G.; Hafner, J. Physical Review B 1993, 47, 558–561.

73. Kresse, G.; Hafner, J. Physical Review B 1994, 49, 14251–14269.

74. Kresse, G.; Furthmüller, J. Physical Review B 1996, 54, 11169–11186.

75. Kresse, G.; Furthmüller, J. Comput. Mater. Sci. 1996, 6, 15–50.

76. Blöchl, P. E. Physical Review B 1994, 50, 17953–17979.

77. Kresse, G.; Joubert, D. Physical Review B 1999, 59, 1758–1775.

78. Perdew, J. P.; Burke, K.; Ernzerhof, M. Physical Review Letters 1996, 77, 3865–3868.

79. Grimme, S.; Antony, J.; Ehrlich, S.; Krieg, H. The Journal of Chemical Physics 2010, 132, 154104.

80. Bučko, T.; Hafner, J.; Lebègue, S.; Ángyán, J. G. The Journal of Physical Chemistry A 2010, 114, 11814–11824.

81. Huang, Y.; Wruss, E.; Egger, D.; Kera, S.; Ueno, N.; Saidi, W.; Bucko, T.; Wee, A.; Zojer, E. Molecules 2014, 19, 2969–2992.

82. Blöchl, P. E.; Jepsen, O.; Andersen, O. K. Physical Review B 1994, 49, 16223–16233.

83. Zaitsev, N. L.; Nechaev, I. A.; Echenique, P. M.; Chulkov, E. V. Physical Review B 2012, 85, 115301.

84. Kügel, J.; Sixta, A.; Böhme, M.; Krönlein, A.; Bode, M. ACS Nano 2016, 10, 11058–11065.

85. Bai, Y.; Buchner, F.; Wendahl, M. T.; Kellner, I.; Bayer, A.; Steinrück, H.-P.; Marbach, H.; Gottfried, J. M. The Journal of Physical Chemistry C 2008, 112, 6087–6092.

86. Nilson, K.; Åhlund, J.; Shariati, M. N.; Schiessling, J.; Palmgren, P.; Brena, B.; Göthelid, E.; Hennies, F.; Huismans, Y.; Evangelista, F. et al. The Journal of Chemical Physics 2012, 137, 044708.

87. Hewson, A. C. Cambridge University Presse, Cambridge, UK 1993, .

88. Nagaoka, K.; Jamneala, T.; Grobis, M.; Crommie, M. F. Physical Review Letters 2002, 88, 1497.

89. Gunnarsson, O.; Schönhammer, K. Physical Review B 1983, 28, 4315–4341.

90. Malterre, D.; Grioni, M.; Baer, Y. Advances in Physics 1996, 45, 299–348.

91. Bickers, N. E.; Cox, D. L.; Wilkins, J. W. Physical Review B 1987, 36, 2036–2079.

92. Patthey, F.; Imer, J.-M.; Schneider, W.-D.; Beck, H.; Baer, Y.; Delley, B. Physical Review B 1990, 42, 8864–8881.

93. Costi, T. A. Physical Review Letters 2000, 85, 1504–1507.

94. Fano, U. Physical Review 1961, 124, 1866–1878.

95. Gruber, M.; Weismann, A.; Berndt, R. Journal of Physics: Condensed Matter 2018, 30, 424001.

96. König, J.; Schoeller, H.; Schön, G. Physical Review Letters 1996, 76, 1715–1718.

97. Flensberg, K. Physical Review B 2003, 68, 205323.

98. Paaske, J.; Flensberg, K. Physical Review Letters 2005, 94, 176801.

99. Chen, Z.-Z.; Lu, H.; Lü, R.; fen Zhu, B. Journal of Physics: Condensed Matter 2006, 18, 5435–5446.

100. Roura-Bas, P.; Tosi, L.; Aligia, A. A. Physical Review B 2013, 87, 195136.

101. Parks, J. J.; Champagne, A. R.; Hutchison, G. R.; Flores-Torres, S.; Abruña, H. D.; Ralph, D. C. Physical Review Letters 2007, 99, 026601.

102. Iancu, V.; Schouteden, K.; Li, Z.; Haesendonck, C. V. Chemical Communications 2016, 52, 11359–11362.

103. Endlich, M.; Gozdzik, S.; Néel, N.; da Rosa, A. L.; Frauenheim, T.; Wehling, T. O.; Kröger, J. The Journal of Chemical Physics 2014, 141, 184308.

104. Li, J.; Schneider, W.-D.; Berndt, R. Physical Review B 1997, 56, 7656–7659.

105. Jeandupeux, O.; Bürgi, L.; Hirstein, A.; Brune, H.; Kern, K. Physical Review B 1999, 59, 15926–15934.

106. Jensen, H.; Kröger, J.; Berndt, R.; Crampin, S. Physical Review B 2005, 71, 155417.

107. Avouris, P.; Lyo, I.-W. Science 1994, 264, 942–945.

108. Li, J.; Schneider, W.-D.; Berndt, R.; Crampin, S. Physical Review Letters 1998, 80, 3332–3335.

109. Tournier-Colletta, C.; Kierren, B.; Fagot-Revurat, Y.; Malterre, D. Physical Review Letters 2010, 104, 016802.

110. Müller, K.; Enache, M.; Stöhr, M. Journal of Physics: Condensed Matter 2016, 28, 153003.

111. Shchyrba, A.; Martens, S. C.; Wäckerlin, C.; Matena, M.; Ivas, T.; Wadepohl, H.; Stöhr, M.; Jung, T. A.; Gade, L. H. Chem. Commun. 2014, 50, 7628–7631.

112. Gross, L.; Moresco, F.; Savio, L.; Gourdon, A.; Joachim, C.; Rieder, K.-H. Physical Review Letters 2004, 93, 2797–4.

113. Iancu, V.; Deshpande, A.; Hla, S.-W. Physical Review Letters 2006, 97, 266603.

114. Klappenberger, F.; Kühne, D.; Krenner, W.; Silanes, I.; Arnau, A.; de Abajo, F. J. G.; Klyatskaya, S.; Ruben, M.; Barth, J. V. Physical Review Letters 2011, 106, 026802.

115. Seufert, K.; Auwärter, W.; de Abajo, F. J. G.; Ecija, D.; Vijayaraghavan, S.; Joshi, S.; Barth, J. V. Nano Letters 2013, 13, 6130–6135.

116. Nicoara, N.; Méndez, J.; Gómez-Rodríguez, J. M. Nanotechnology 2016, 27, 475707.

117. Heller, E. J.; Crommie, M. F.; Lutz, C. P.; Eigler, D. M. Nature 1994, 369, 464–466.

118. Bidermane, I.; Brumboiu, I. E.; Totani, R.; Grazioli, C.; Shariati-Nilsson, M. N.; Herper, H. C.; Eriksson, O.; Sanyal, B.; Ressel, B.; de Simone, M. et al. Journal of Electron Spectroscopy and Related Phenomena 2015, 205, 92–97.

119. Gerber, I. C.; Poteau, R. Theoretical Chemistry Accounts 2018, 137, 156.

120. Minamitani, E.; Nakanishi, H.; Diño, W. A.; Kasai, H. Solid State Communications 2009, 149, 1241–1243.

121. Jayaprakash, C.; Krishna-murthy, H. R.; Wilkins, J. W. Physical Review Letters 1981, 47, 737–740.

122. Ashcroft, N. W.; Mermin, N. D. Saunders 1976, .

123. Li, Q. L.; Zheng, C.; Wang, R.; Miao, B. F.; Cao, R. X.; Sun, L.; Wu, D.; Wu, Y. Z.; Li, S. C.; Wang, B. G. et al. Physical Review B 2018, 97, 035417.

124. Limot, L.; Berndt, R. Applied Surface Science 2004, 237, 572–576.

125. Moro-Lagares, M.; Fernández, J.; Roura-Bas, P.; Ibarra, M. R.; Aligia, A. A.; Serrate, D. Physical Review B 2018, 97, 235442.

126. Bao, D.-L.; Zhang, Y.-Y.; Du, S.; Pantelides, S. T.; Gao, H.-J. The Journal of Physical Chemistry C 2018, 122, 6678–6683.

Supporting Information Available

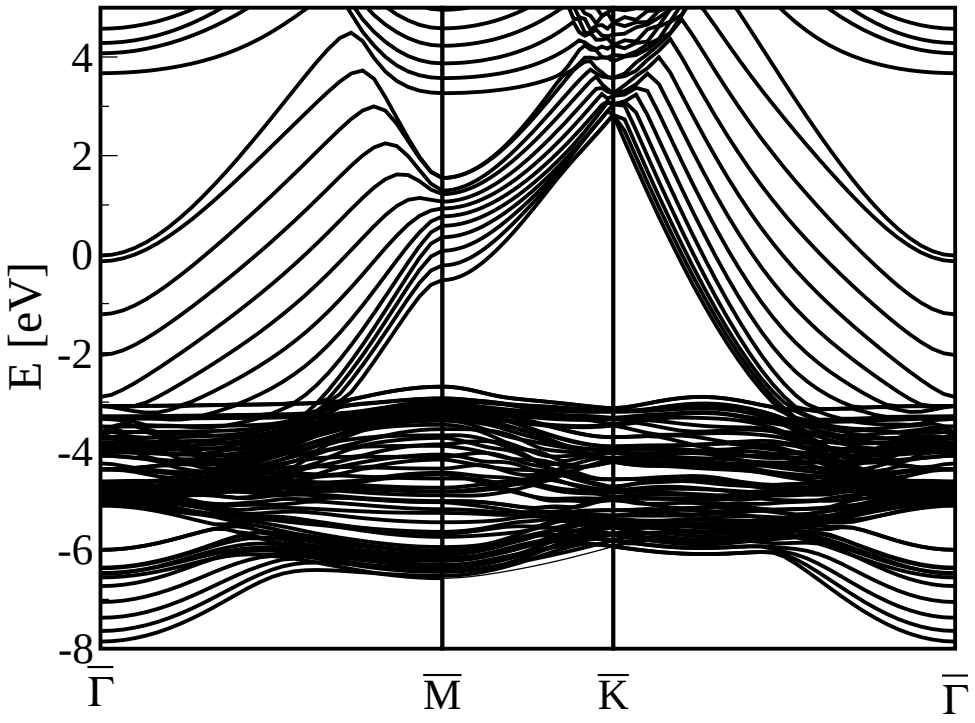

Figure 6: Calculated band structure of the 12-layers slab of Ag in its primitive cell.

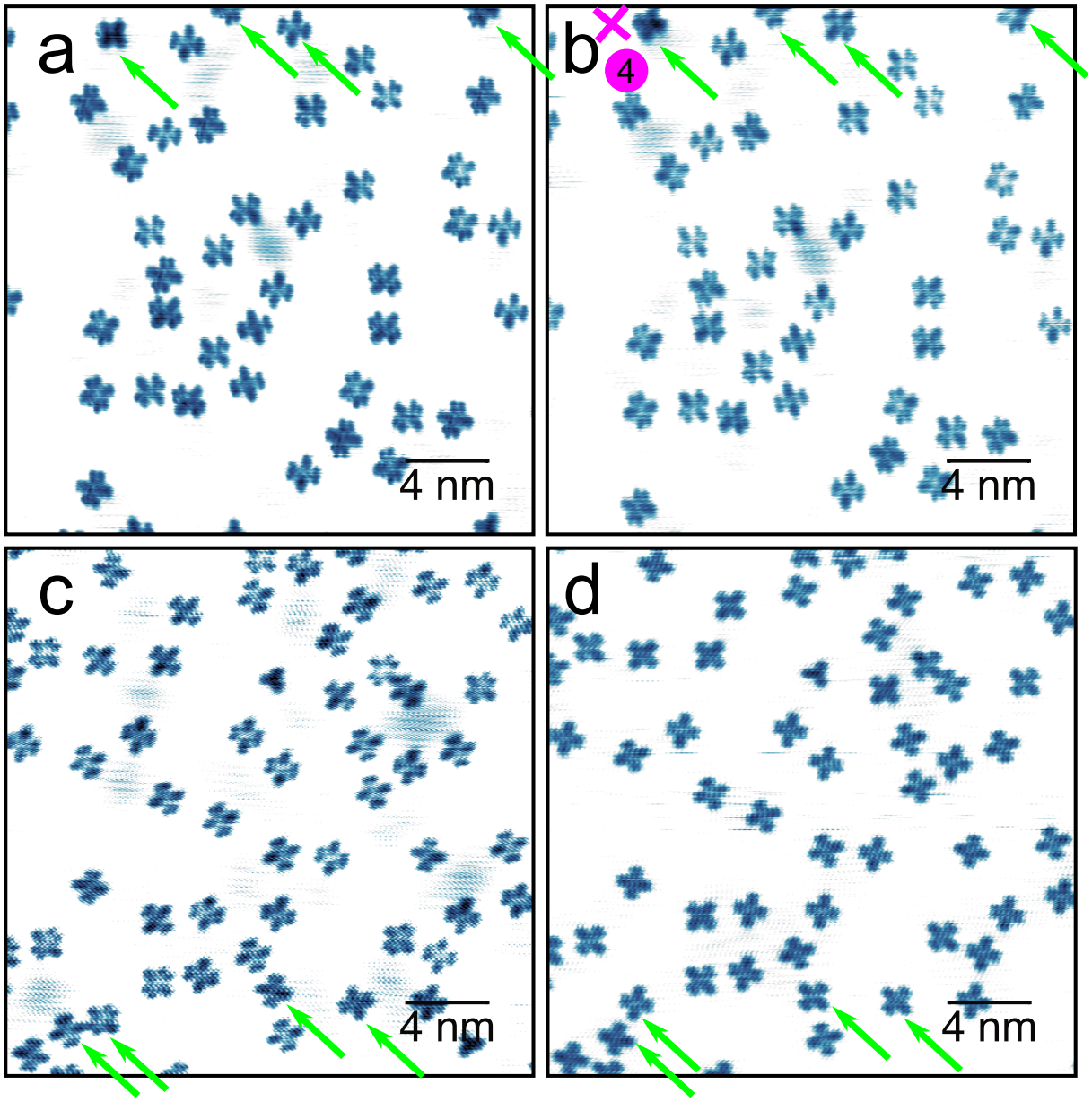

Figure 7: Pairs of STM images recorded successively (a,b) and (c,d). Tunneling current: 200 pA. Bias voltage: (a) 1 mV, (b) 7 mV,(c) −7 mV and (d) 100 mV. Green arrows point to molecules that have rotated between scans. The color scale is such that dark blue colors represent high z values. The cross in (b) corresponds to spectrum number 4 in Fig.4(a).

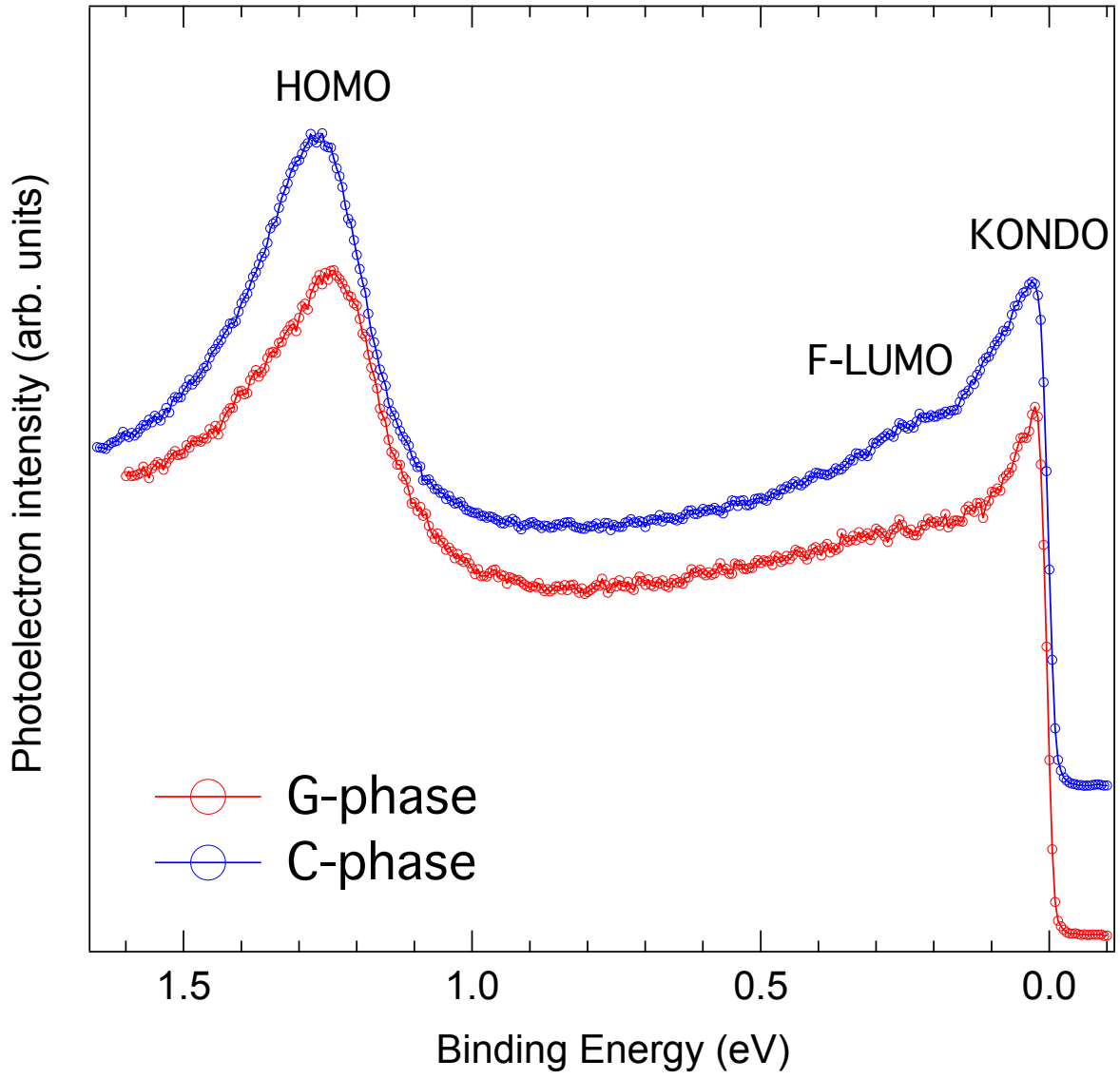

Figure 8: UPS spectra recorded at T= 9 K on G and C-phases. Spectra have been shifted vertically for clarity.

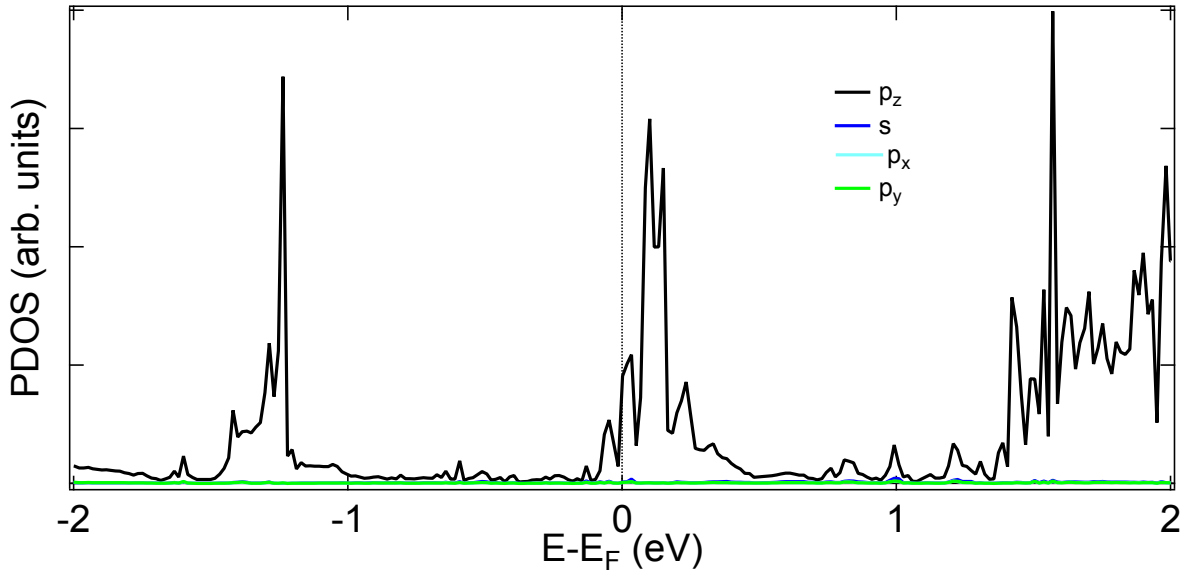

Figure 9: (a) Computed density of states projected onto atomic orbitals of 2HPc on Ag(111) for molecules arranged in 7×7 arrangement.

This material is available free of charge via the Internet at `http://pubs.acs.org/`.

Graphical TOC Entry

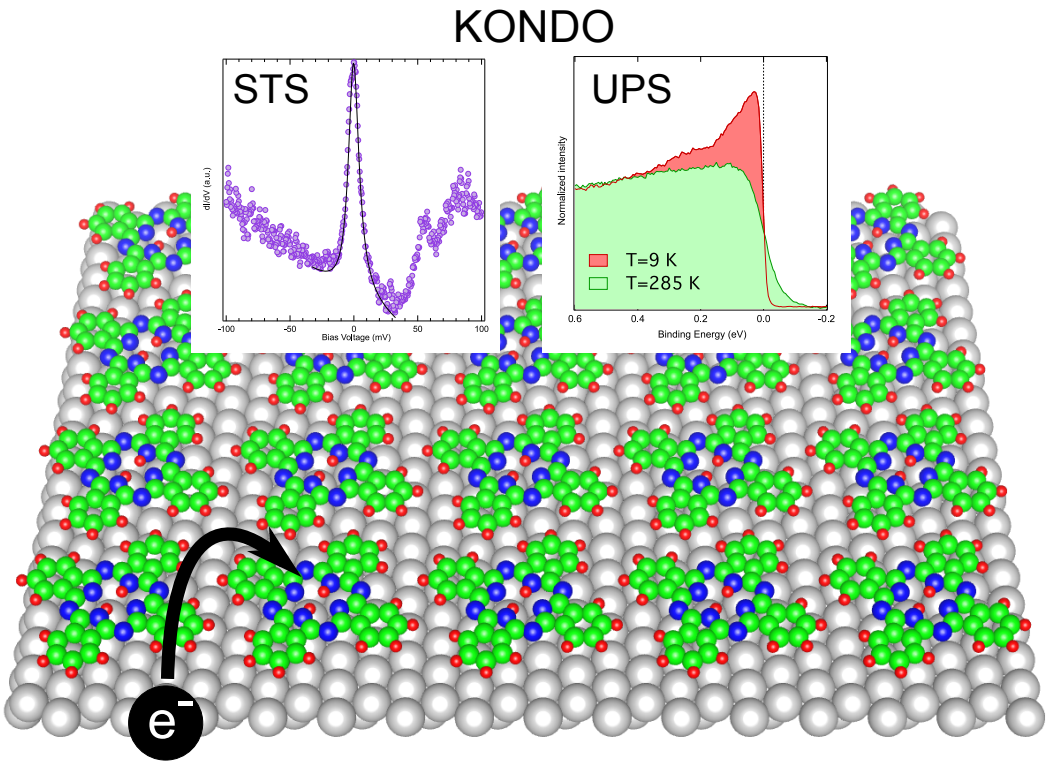

Figure 10: Figure TOC